

Smoothed SVD-based Beamforming for FBMC/OQAM Systems Based on Frequency Spreading

Yu Qiu, Daiming Qu, Da Chen, and Tao Jiang, *Senior Member, IEEE*

Abstract—The combination of singular value decomposition (SVD)-based beamforming and filter bank multicarrier with offset quadrature amplitude modulation (FBMC/OQAM) has not been successful to date. The difficulty of this combination is that, the beamformers may experience significant changes between adjacent subchannels, therefore destroy the orthogonality among FBMC/OQAM real-valued symbols, even under channels with moderate frequency selectivity. In this paper, we address this problem from two aspects: i) an SVD-FS-FBMC architecture is adopted to support beamforming with finer granularity in frequency domain, based on the frequency spreading FBMC (FS-FBMC) structure, i.e., beamforming on FS-FBMC tones rather than on subchannels; ii) criterion and methods are proposed to smooth the beamformers from tone to tone. The proposed finer beamforming and smoothing greatly improve the smoothness of beamformers, therefore effectively suppress the leaked ICI/ISI. Simulations are conducted under the scenario of IEEE 802.11n wireless LAN. Results show that the proposed SVD-FS-FBMC system shares close BER performance with its orthogonal frequency division multiplexing (OFDM) counterpart under the frequency selective channels.

Index Terms—Filter bank multicarrier (FBMC), frequency spreading FBMC (FS-FBMC), MIMO, precoding, singular value decomposition (SVD), frequency selective channel.

I. INTRODUCTION

Filter bank multicarrier with offset quadrature amplitude modulation (FBMC/OQAM) [1]–[12] is considered as a promising alternative to the conventional orthogonal frequency division multiplexing (OFDM) technique [13], [14]. However, integration of multiple-input multiple-output (MIMO) techniques with FBMC/OQAM, in general, is more complicated than with OFDM. Thanks to the adding of CP, a subchannel (subcarrier band) is exactly flat and independent from other subchannels in OFDM systems. Thus, MIMO precoding and equalization can be taken on each subchannel independently, without leading to any inter-carrier interference (ICI) or inter-symbol interference (ISI). However, without CP, the MIMO precoding and equalization of FBMC systems are more complicated and could lead to considerable ICI/ISI under frequency selective channels, due to the fact that FBMC/OQAM

is a non-orthogonal waveform (FBMC/OQAM symbols are orthogonal with each other only in the real domain [1]–[3]).

In FBMC/OQAM systems, the real and imaginary parts of QAM symbol are separated and transmitted as pulse amplitude modulated (PAM) symbols. There exists ICI/ISI interference between the PAM symbols in the form of imaginary interference. ICI/ISI-free symbols are obtained only after channel equalization and taking the real parts, e.g., see [1]–[3], [10] for details. The combination of MIMO and FBMC/OQAM is a trivial task in channels with high coherence bandwidth, which is almost equivalent to MIMO-OFDM systems. While for the frequency selective channels, without carefully design, the beamforming matrices could differ dramatically between adjacent subchannels, and the imaginary interference from one subchannel could be leaked into adjacent subchannels as real interference, therefore destroy the orthogonality among FBMC/OQAM PAM symbols in the real domain [15].

Aware of the ICI/ISI interference, some studies [16]–[20] attempt to constrain this interference by careful design of precoding as well as equalization for MIMO-FBMC/OQAM systems. In [16], two MIMO-FBMC precoding/equalization schemes were designed to maximize the signal to leakage plus noise ratio (SLNR) and the signal to interference plus noise ratio (SINR), respectively. Criterion of minimizing the sum mean square error was adopted in [17]. The coordinated beamforming technique was applied in MIMO-FBMC/OQAM systems [18], where the precoding and decoding matrix are computed jointly and iteratively. A two-step method was proposed in [19], where the precoders are first optimized to maximize the SLNR given the equalizers and then, the equalizers are designed according to the minimum mean square error (MMSE) criterion while fixing the precoders. Although the ICI/ISI interference is suppressed, error performance loss or significantly increased complexity, compared with their OFDM counterparts, are observed with the aforementioned MIMO-FBMC/OQAM schemes. Very recently, a novel architecture was proposed to approximate an ideal frequency selective precoder and linear receiver by Taylor expansion, exploiting the structure of the analysis and synthesis filter banks [21]. This architecture was shown to be very promising, however more results are needed to reveal its full potential. Smoothing of the precoders is proposed in [22], which keeps the phase of one precoder component constant across subcarriers. However, the phase continuity criterion is not effective when this precoder component crosses zero and changes its sign. A more thorough review of MIMO-FBMC/OQAM

Yu Qiu, Daiming Qu (corresponding author), Da Chen, and Tao Jiang are with the School of Electronics Information and Communications, Huazhong University of Science and Technology, Wuhan, 430074, P. R. China (e-mail: qudaiming@hust.edu.cn).

This work is supported in part by the National Natural Science Foundation of China (61571200, 61701186) and the open research fund of National Mobile Communications Research Laboratory, Southeast University (2014D09).

precoding/beamforming techniques, including those for multi-user MIMO [23]–[25], could be found in [26].

Most of the works on precoding/beamforming of MIMO-FBMC under frequency selective channels assume ployphase network implementation of FBMC [27], [28]. In this paper, we focus on another type of implementation, namely frequency spreading FBMC (FS-FBMC), which has attracted wide attention in recent years [30]–[41]. MIMO methods specifically designed for this type of implementation are in need.

Singular value decomposition (SVD) based beamforming, adopted in the IEEE 802.11n wireless LAN standard, yields maximum likelihood performance with simple linear transmit and receive beamformers for MIMO-OFDM systems [29]. Unfortunately, perfect combination with SVD beamforming is not yet available for FBMC/OQAM systems. In this paper, we propose a novel SVD-FS-FBMC scheme that is robust to channel frequency selectivity. While traditional beamforming of MIMO-FBMC are taken on per-subchannel basis, the proposed scheme enables beamforming of finer granularity in frequency by using the frequency spreading FBMC (FS-FBMC) structure [30]–[34], i.e., beamforming on FS-FBMC tones. We further propose two methods, namely phase factor optimization and orthogonal iteration, to smooth the SVD-based beamformers from tone to tone. The criterion of smoothing proposed is to minimize the Euclidean distance between adjacent beamformers. The proposed finer beamforming and smoothing methods greatly improve the smoothness of beamformers, therefore effectively suppress the leaked ICI/ISI from adjacent subchannels. Simulations are conducted under the scenario of IEEE 802.11n wireless LAN and the results show that the proposed SVD-FS-FBMC system performs closely with its OFDM counterpart under the IEEE 802.11n Channel Models. Our preliminary results on this subject have been reported in [34].

The following notations are used in this paper. Bold lower-case letters denote column vectors. Bold upper-case letters are used for matrices. The superscripts $(\cdot)^T$, $(\cdot)^*$, $(\cdot)^H$, and $(\cdot)^\dagger$ represent the transpose, conjugate, Hermitian transpose, and Moore-Penrose pseudo-inverse, respectively. $\Re\{\cdot\}$ and $\Im\{\cdot\}$ denote the real and imaginary parts, respectively. $\mathbb{E}[\cdot]$ stands for the expectation. $\|\cdot\|_2$ denotes vector or matrix 2-norm, $\|\cdot\|_F$ denotes the matrix Frobenius-norm, whenever the particular choice of norm is unimportant, $\|\cdot\|$ is used. Function \sin and \arccos of a matrix is applied element-wisely in this paper. Finally, $j = \sqrt{-1}$.

II. SYSTEM MODELS & ICI/ISI OF SVD-FBMC/OQAM

A. FBMC/OQAM System Model

Fig. 1 presents the equivalent baseband block diagram of an FBMC/OQAM system. It consists of M subcarriers with subcarrier spacing $1/T$, where T is the interval between the complex-valued symbols in time. Each complex-valued symbol is partitioned into a pair of real-valued PAM symbols. The PAM symbol at the frequency-time index (m, n) is denoted by $a_{m,n}$, where m is the frequency/subchannel index and n is the time index. Moreover, $a_{m,2\hat{n}}$ and $a_{m,2\hat{n}+1}$, with integer \hat{n} , are real and imaginary parts of a QAM symbol

and are $T/2$ spaced in time. With a sampling interval of T/M , the filter bank prototype filter has the discrete time impulse response $g(i)$, which we assume only have non-zero coefficients for $0 < i \leq KM-1$, where K is a positive integer. We further assume that $g(i)$ is an even-symmetric pulse, i.e., $g(i) = g(KM-i)$.

The discrete-time baseband equivalent of an FBMC/OQAM signal may be presented as [2], [42]

$$x(i) = \sum_{m=0}^{M-1} \sum_{n \in \mathbb{Z}} a_{m,n} \underbrace{g(i - n\frac{M}{2}) e^{j\frac{2\pi mi}{M}} e^{j\frac{\pi(m+n)}{2}}}_{g_{m,n}(i)}, \quad (1)$$

where $g_{m,n}(i)$ is the pulse of the (m, n) -th PAM symbol. When an FBMC/OQAM signal is transmitted through a channel that varies slowly with time and its delay spread is significantly shorter than the symbol interval, the channel transfer function over each subchannel may be approximated by a flat gain. Let $H_{m,n}$ denote this gain for the m -th subchannel at the n -th time index. With the slow varying assumption, we omit the subscript n from $H_{m,n}$ for simplicity of presentation. Then, the m_0 th output of the receiver analysis filter bank at the n_0 th time index is obtained as, [2], [42],

$$\begin{aligned} r_{m_0, n_0} &= \sum_{i=-\infty}^{\infty} g_{m_0, n_0}^*(i) \sum_{m=0}^{M-1} \sum_{n \in \mathbb{Z}} H_m a_{m,n} g_{m,n}(i) \\ &\approx H_{m_0} a_{m_0, n_0} + H_{m_0} \sum_{(m,n) \neq (m_0, n_0)} a_{m,n} \zeta_{m,n}^{m_0, n_0} \end{aligned} \quad (2)$$

where

$$\zeta_{m,n}^{m_0, n_0} = \sum_{i=-\infty}^{\infty} g_{m_0, n_0}^*(i) g_{m,n}(i). \quad (3)$$

It is noteworthy that for a well-designed prototype filter $g(i)$, $\zeta_{m,n}^{m_0, n_0} = 1$ when $(m, n) = (m_0, n_0)$, and is zero or a pure imaginary value when $(m, n) \neq (m_0, n_0)$, e.g., see [1]. To be more specific, $\zeta_{m,n}^{m_0, n_0}$, for $(m, n) \neq (m_0, n_0)$, represents the imaginary interference to $a_{m,n}$, which could be removed by taking the real part after channel equalization.

B. SVD-based MIMO Beamforming

We consider a MIMO system equipped with N_t transmit antennas and N_r receive antennas, which supports L parallel streams. The SVD decomposition of the channel $\mathbf{H} \in \mathbb{C}^{N_r \times N_t}$ is:

$$\mathbf{H} = \mathbf{U} \mathbf{D} \mathbf{V}^H, \quad (4)$$

where $\mathbf{V} \in \mathbb{C}^{N_t \times N_t}$ and $\mathbf{U} \in \mathbb{C}^{N_r \times N_r}$ are unitary matrices, and \mathbf{D} is an N_r -by- N_t rectangular diagonal matrix containing $(\lambda^1, \lambda^2 \dots)$ as diagonal elements, where $\lambda^1, \lambda^2 \dots$ denote the singular values that are sorted in descending order and are real-valued. When $L = N_t = N_r$, the transmit beamformer and receive beamformer are simply \mathbf{V} and \mathbf{U}^H , respectively. When $L < N_t$ or $L < N_r$, they are submatrices of \mathbf{V} and \mathbf{U}^H , respectively, corresponding to the L largest singular values. For clarity of notations, we abuse the notations \mathbf{V} and/or \mathbf{U}^H and let them also represent the beamformers when $L < N_t$ or $L < N_r$ in the rest of this paper, then $\mathbf{V} \in \mathbb{C}^{N_t \times L}$ and

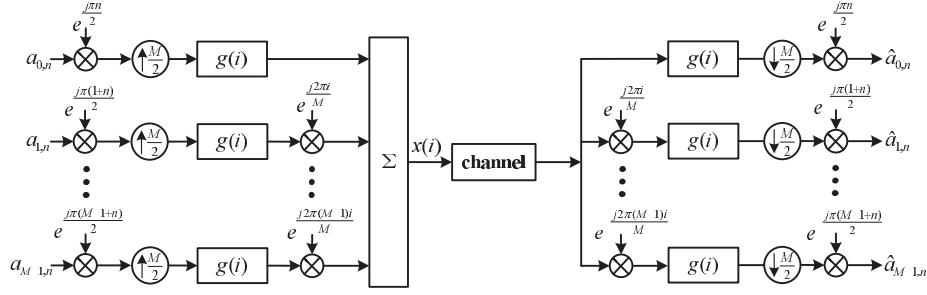


Fig. 1. The equivalent baseband block diagram of an FBMC/OQAM system.

$\mathbf{U}^H \in \mathbb{C}^{L \times N_r}$. With the transmit beamforming and MIMO channel, the signal at the receiver is

$$\mathbf{y} = \mathbf{H}\mathbf{V}\mathbf{s} + \mathbf{n}, \quad (5)$$

where \mathbf{s} is the symbols to be transmitted and \mathbf{n} is the receive noise vector (\mathbf{y} , \mathbf{s} and \mathbf{n} are $N_r \times 1$, $L \times 1$ and $N_r \times 1$ vectors, respectively). The signal after receive beamforming is

$$\mathbf{r} = \mathbf{U}^H \mathbf{y} = \mathbf{U}^H (\mathbf{H}\mathbf{V}\mathbf{s} + \mathbf{n}) = \mathbf{D}\mathbf{s} + \tilde{\mathbf{n}}, \quad (6)$$

where $\tilde{\mathbf{n}} = \mathbf{U}^H \mathbf{n}$ (\mathbf{r} and $\tilde{\mathbf{n}}$ are $L \times 1$ vectors). Clearly, the transmitted symbols are recovered with nonequal gains [43], and there is no interference among streams.

C. Straightforward Combination of SVD and FBMC/OQAM

In this subsection, we present the model of straightforward combination of SVD and FBMC/OQAM and discuss about the interference leakage problem. Combining the models in subsection II-A and II-B, the transmitted signal of the SVD-FBMC/OQAM is represented by a sequence of vectors $\mathbf{x}(i) = [x_1(i) \ x_2(i) \ \cdots \ x_{N_t}(i)]^T$ as

$$\mathbf{x}(i) = \sum_{m=0}^{M-1} \sum_{n \in \mathbb{Z}} \mathbf{V}_m \mathbf{a}_{m,n} g_{m,n}(i), \quad (7)$$

where $\mathbf{a}_{m,n} = [a_{m,n}^1 \ a_{m,n}^2 \ \cdots \ a_{m,n}^L]^T$ is the symbol vector to be transmitted, and $g_{m,n}(i)$ is the frequency-time shifted version of prototype filter $g(i)$ (see (1)), $\mathbf{V}_m \in \mathbb{C}^{N_t \times L}$ denotes the beamforming matrix for the m -th subchannel. Assuming nearly flat fading across the subcarrier band (the bandwidth of subchannel), the received signal at the output of analysis filters for Time n_0 and Subchannel m_0 is

$$\begin{aligned} \mathbf{r}_{m_0, n_0} &\approx \sum_{m=0}^{M-1} \sum_{n \in \mathbb{Z}} \mathbf{U}_{m_0}^H \mathbf{H}_m \mathbf{V}_m \mathbf{a}_{m,n} \sum_{i=-\infty}^{\infty} g_{m_0, n_0}^*(i) g_{m,n}(i) \\ &= \sum_{m=0}^{M-1} \sum_{n \in \mathbb{Z}} \mathbf{U}_{m_0}^H \mathbf{H}_m \mathbf{V}_m \mathbf{a}_{m,n} \zeta_{m,n}^{m_0, n_0} \\ &= \mathbf{D}_{m_0} \mathbf{a}_{m_0, n_0} \\ &\quad + \sum_{(m,n) \neq (m_0, n_0)} \mathbf{U}_{m_0}^H \mathbf{H}_m \mathbf{V}_m \mathbf{a}_{m,n} \zeta_{m,n}^{m_0, n_0}, \end{aligned} \quad (8)$$

where $\mathbf{H}_m \in \mathbb{C}^{N_r \times N_t}$ is the MIMO channel response of Subchannel m , $\mathbf{U}_{m_0}^H \in \mathbb{C}^{L \times N_r}$ is the receive beamformer for the m_0 -th subchannel. Clearly, the first term of (8) is

the recovered symbols and the second term is the ICI/ISI interference. If $\mathbf{H}_{m_0} \approx \mathbf{H}_m$ and $\mathbf{V}_{m_0} \approx \mathbf{V}_m$ for subchannels adjacent to m_0 , we have $\mathbf{U}_{m_0}^H \mathbf{H}_m \mathbf{V}_m \approx \mathbf{D}_{m_0}$, and the ISI/ICI term is approximately imaginary and could be removed by taking the real part of \mathbf{r}_{m_0, n_0} (recall that \mathbf{D}_{m_0} is real-valued). However, this does not work even under channels with moderate frequency selectivity. The reason is that: the transmit and receive beamformer may experience significant changes between adjacent subchannels due to channel variation, then $\mathbf{U}_{m_0}^H \mathbf{H}_m \mathbf{V}_m$ is not real-valued and the ISI/ICI term is no longer pure imaginary, which results in leaked ICI/ISI interference into the real part of \mathbf{r}_{m_0, n_0} .

III. THE FINER BEAMFORMING ARCHITECTURE

In this section, we propose finer beamforming for FBMC/OQAM, here finer beamforming means beamforming with finer granularity in frequency domain. As discussed in the above section, the straightforward SVD-FBMC/OQAM systems beamform at the subchannel level, i.e., each subchannel has its own transmit and receive beamformer. To enable a finer granularity, we adopt the FS-FBMC structure [30]–[33], and beamformers are designed at each tone of FS-FBMC. The proposed finer beamforming provides a basic architecture to support smoother changes from subchannel to subchannel.

A. Frequency Spreading FBMC (FS-FBMC)

The FS-FBMC structure, a special form of the fast convolution implementation of filter banks [44]–[49], uses frequency spreading/despreading to implement the filtering in the frequency domain for FBMC/OQAM systems. In FS-FBMC, FFT/IFFT is taken at the length of KM . Let $G(k)$ denote the FFT of a segment of $g(i)$ in the range of $0 \leq i \leq KM - 1$, where $0 \leq k \leq KM - 1$ is the index of FS-FBMC tones. We assume that $G(k)$ has $2P - 1$ non-negligible tones that center around the zero-th tone, where P is a positive integer. Let $G_{m,n}^{(n_0)}(k)$ denote the FFT of a segment of $g_{m,n}(i)$ in the range of $n_0 M/2 \leq i \leq n_0 M/2 + KM - 1$, which is the portion of $g_{m,n}(i)$ that falls inside the n_0 -th sliding window. The superscript (n_0) is to emphasize that the FFT is taken at the n_0 -th window. Then, the filtering at the n -th time index is implemented in the frequency domain by spreading the PAM symbols with $G_{m,n}^{(n)}(k)$ as

$$b_n(k) = \sum_{m=0}^{M-1} a_{m,n} G_{m,n}^{(n)}(k), \quad (9)$$

where $G_{m,n}^{(n)}(k)$ is the FFT of the non-zero part of pulse $g_{m,n}(i)$, i.e., at the n -th window. And, the output of the frequency spreading is fed to the IFFT transformation to obtain the time domain samples of the n -th time index as

$$x_n(i) = \begin{cases} \sum_{k=0}^{KM-1} b_n(k) e^{j\frac{2\pi k(i-nM/2)}{KM}}, & \frac{nM}{2} \leq i \leq \frac{nM}{2} + KM - 1 \\ 0, & \text{else} \end{cases}. \quad (10)$$

Then, the transmitted time sequence is obtained by accumulation over all symbols as

$$x(i) = \sum_{n \in \mathbb{Z}} x_n(i). \quad (11)$$

At the receiver, a sliding window is employed to select KM samples every $M/2$ samples, which are fed to an FFT module. Then, the transmitted PAM symbols are recovered through equalization and frequency despreading. More details of FS-FBMC transmission could be found in [50].

B. Finer SVD Beamforming

Fig. 2 presents the transmitter of the proposed finer SVD-FS-FBMC, where $\mathbf{V}_k \in \mathbb{C}^{N_t \times L}$ is the beamforming matrix for the k -th FS-FBMC tone, and $\mathbf{V}_k = [\mathbf{v}_k^1 \ \mathbf{v}_k^2 \ \dots \ \mathbf{v}_k^L]$, here \mathbf{v}_k^l denotes the beamforming vector for the l -th stream. The beamformed signals on all transmit antennas for the k -th tone and n -th time index is given by an N_t -by-1 vector

$$\mathbf{b}_n(k) = \mathbf{V}_k \sum_{m=0}^{M-1} \mathbf{a}_{m,n} G_{m,n}^{(n)}(k). \quad (12)$$

Then, the samples on all transmit antennas for the n -th time index is obtained by IFFT

$$\mathbf{x}_n(i) = \begin{cases} \sum_{k=0}^{KM-1} \mathbf{b}_n(k) e^{j\frac{2\pi k(i-nM/2)}{KM}}, & \frac{nM}{2} \leq i \leq \frac{nM}{2} + KM - 1 \\ 0, & \text{else} \end{cases}, \quad (13)$$

where $\mathbf{x}_n(i)$ is an N_t -by-1 vector.

After accumulation over all symbols, the transmitted signals on all antennas are represented by the following vector sequence

$$\mathbf{x}(i) = \sum_{n \in \mathbb{Z}} \mathbf{x}_n(i). \quad (14)$$

Fig. 3 presents the receiver of the proposed SVD-FS-FBMC, where $\mathbf{U}_k^H \in \mathbb{C}^{L \times N_r}$ is the beamforming matrix for the k -th FS-FBMC tone, and $\mathbf{U}_k^H = [(\mathbf{u}_k^1)^H \ (\mathbf{u}_k^2)^H \ \dots \ (\mathbf{u}_k^L)^H]$, here $(\mathbf{u}_k^l)^H$ denotes the receive beamforming vector for the l -th stream. Let N_r -by-1 vector $\mathbf{y}(i)$ denote the i -th received samples on all receive antennas, and $\mathbf{y}^{(n_0)}(i)$ ($0 \leq i \leq KM - 1$) denote the selected KM samples by the n_0 -th sliding window, i.e.,

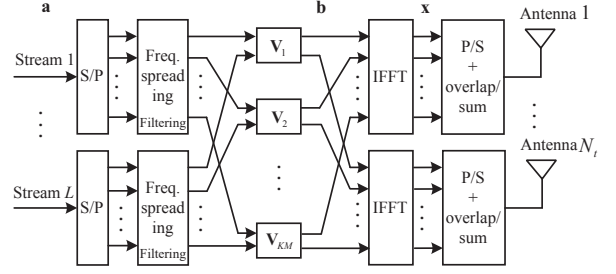


Fig. 2. The transmitter of the proposed SVD-FS-FBMC scheme.

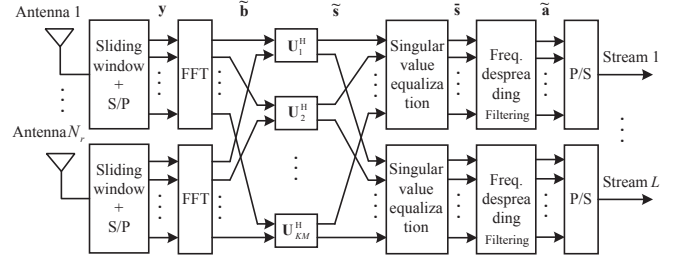


Fig. 3. The receiver of the proposed SVD-FS-FBMC scheme.

$\mathbf{y}^{(n_0)}(i) = \mathbf{y}(i + n_0M/2)$, for $0 \leq i \leq KM - 1$. Taking FFT of $\mathbf{y}^{(n_0)}(i)$, we obtain

$$\tilde{\mathbf{b}}^{(n_0)}(k) = \frac{1}{KM} \sum_{i=0}^{KM-1} \mathbf{y}^{(n_0)}(i) e^{-j\frac{2\pi ki}{KM}}, 0 \leq k \leq KM - 1. \quad (15)$$

Applying the receive beamformer, we have the signals received on the k -th tone

$$\tilde{\mathbf{s}}^{(n_0)}(k) = \mathbf{U}_k^H \tilde{\mathbf{b}}^{(n_0)}(k), \quad (16)$$

where $\tilde{\mathbf{s}}^{(n_0)}(k)$ is an L -by-1 vector that holds the samples of all streams. Noting that different tones and streams may have different singular values, an equalizer is required at each tone for each stream. The equalizers for the k -th tone is represented by an L -by- L diagonal matrix $\mathbf{E}_k = \text{diag}\{E_k^1, E_k^2, \dots, E_k^L\}$, where E_k^l is the equalizer for Stream l and Tone k . If it is a zero forcing (ZF) equalization, $E_k^l = 1/\lambda_k^l$. Then, the equalized signal is obtained as

$$\tilde{\mathbf{s}}^{(n_0)}(k) = \mathbf{E}_k \tilde{\mathbf{s}}^{(n_0)}(k). \quad (17)$$

Finally, despreading is applied to obtain the PAM symbols at the m_0 -th subchannel and n_0 -th time index

$$\begin{aligned} \tilde{\mathbf{a}}_{m_0, n_0} &= \sum_{k=0}^{KM-1} G_{m_0, n_0}^{(n_0)*}(k) \tilde{\mathbf{s}}^{(n_0)}(k) \\ &= \sum_{k=0}^{KM-1} G_{m_0, n_0}^{(n_0)*}(k) \mathbf{E}_k \mathbf{U}_k^H \tilde{\mathbf{b}}^{(n_0)}(k). \end{aligned} \quad (18)$$

Under the assumption that \mathbf{E}_k , \mathbf{U}_k , \mathbf{H}_k and \mathbf{V}_k are nearly flat, i.e., they vary slowly, across the subcarrier band,

$$\begin{aligned} & \tilde{\mathbf{a}}_{m_0, n_0} \\ \approx & \mathbf{a}_{m_0, n_0} + \sum_{(m, n) \neq (m_0, n_0)} \mathbf{a}_{m, n} \sum_{k=0}^{KM-1} \zeta_{m, n}^{m_0, n_0} \\ & + \sum_{k=0}^{KM-1} G_{m_0, n_0}^{(n_0)*}(k) \mathbf{E}_k \mathbf{U}_k^H \mathbf{n}^{(n_0)}(k), \end{aligned} \quad (19)$$

where $\mathbf{n}^{(n_0)}(k)$ is FFT of the noise with $\mathbf{y}^{(n_0)}(i)$. Proof of this equation is presented in the Appendix. Clearly, the first term of (19) is the transmitted PAM symbols, and the second term is the ICI/ISI interference that is pure imaginary under the nearly-flat assumption and could be removed by taking the real part.

Obviously, the complexity of beamforming in the proposed SVD-FS-FBMC system is roughly proportional to the number of tones per subchannel, i.e. K . When $K = 1$, i.e. without frequency spreading and despreading, the proposed SVD-FS-FBMC is exactly the same as that of SVD-OFDM with the same subchannel number M . Therefore, the complexity of beamforming in the proposed SVD-FS-FBMC is K times that of the SVD-OFDM with the same subchannel number M .

Compared with the straightforward SVD-FBMC/OQAM given in Section II-C, the major improvement by the finer beamforming is that it allows smoother transition of beamformers.

IV. BOUNDS ON THE EUCLIDEAN DISTANCE BETWEEN ADJACENT BEAMFORMING MATRICES

The derivation of the finer SVD-FS-FBMC in Subsection III-B is under the assumption that \mathbf{H}_k is nearly flat across the subcarrier bandwidth, as well as \mathbf{E}_k , \mathbf{U}_k and \mathbf{V}_k . In this section, we will show that \mathbf{E}_k , \mathbf{U}_k and \mathbf{V}_k that are nearly flat are available, i.e., they can be bounded in Euclidean distance between adjacent tones, as long as \mathbf{H}_k is nearly flat. The reasoning here is based on the perturbation theory for SVD decomposition [54]–[56].

This section also serves as a justification to the smoothing criterion proposed in Section V, which minimizes the Euclidean distance between beamformers of adjacent tones.

As the channel is assumed to be nearly flat, \mathbf{H}_k can be written as

$$\mathbf{H}_k = \mathbf{H}_{k-1} + \Delta \mathbf{H}_k, \quad (20)$$

where $\Delta \mathbf{H}_k$ is an N_r -by- N_t matrix, and $\|\Delta \mathbf{H}_k\|_2 \ll \|\mathbf{H}_{k-1}\|_2$. Then, the Weyl theorem [55] gives a bound on the difference between the singular values of \mathbf{H}_k and \mathbf{H}_{k-1} .

Theorem 1 (Weyl).

$$|\lambda_k^l - \lambda_{k-1}^l| \leq \|\Delta \mathbf{H}_k\|_2, \quad l = 1, \dots, L. \quad (21)$$

Due to the Weyl theorem, when $\|\Delta \mathbf{H}_k\|_2$ is small, the difference between λ_k^l and λ_{k-1}^l is also small. Thus, \mathbf{E}_k can be assumed nearly flat.

To bound the difference between \mathbf{V}_k and \mathbf{V}_{k-1} as well as that between \mathbf{U}_k and \mathbf{U}_{k-1} , we take use of the Wedin theorem

[56] below. With the Wedin's theorem, we will show that the eigenspaces spanned by \mathbf{V}_k^l and \mathbf{V}_{k-1}^l are close, where $\mathbf{V}_k^l = [\mathbf{v}_k^1, \dots, \mathbf{v}_k^l]$. We will also show that \mathbf{V}_k^{l-1} and \mathbf{V}_{k-1}^{l-1} are close. Then, we reach the conclusion that the eigenspaces spanned by \mathbf{v}_k^l and \mathbf{v}_{k-1}^l are close. Similarly, subspaces \mathbf{u}_k^l and \mathbf{u}_{k-1}^l are close as well.

In stead of directly bounding the Euclidean distance between the singular vectors, the Wedin theorem gives a bound on angles between the subspaces spanned by the singular vectors. Let \mathbf{L} and \mathbf{M} in $\mathbb{C}^{N \times l}$ have full column rank l , the angle matrix from \mathbf{L} to \mathbf{M} is defined as [56]

$$\begin{aligned} \Theta(\mathbf{L}, \mathbf{M}) &= \\ & \arccos((\mathbf{L}^H \mathbf{L})^{-\frac{1}{2}} \mathbf{L}^H \mathbf{M} (\mathbf{M}^H \mathbf{M})^{-1} \mathbf{M}^H \mathbf{L} (\mathbf{L}^H \mathbf{L})^{-\frac{1}{2}})^{-\frac{1}{2}}. \end{aligned}$$

Then, $\|\sin \Theta(\mathbf{L}, \mathbf{M})\|_F$ gives a measure of how much the subspaces of \mathbf{L} and \mathbf{M} are separated in angle [56]. With the definition, the Wedin theorem is given as

Theorem 2 (Wedin). *If there is a $\delta > 0$, such that*

$$\min_{1 \leq i \leq l, j \geq l+1} |\lambda_k^i - \lambda_{k-1}^j| \geq \delta, \quad (22)$$

and

$$\lambda_k^l \geq \delta, \quad (23)$$

then

$$\begin{aligned} & \sqrt{\|\sin \Theta(\mathbf{V}_k^l, \mathbf{V}_{k-1}^l)\|_F^2 + \|\sin \Theta(\mathbf{U}_k^l, \mathbf{U}_{k-1}^l)\|_F^2} \\ & \leq \frac{\sqrt{\|\mathbf{R}_R^l\|_F^2 + \|\mathbf{R}_L^l\|_F^2}}{\delta}, \end{aligned} \quad (24)$$

where

$$\begin{aligned} \mathbf{R}_R^l &= \mathbf{H}_{k-1} \mathbf{V}_k^l - \mathbf{U}_k^l \text{Diag}(\lambda_k^1, \dots, \lambda_k^l) \\ \mathbf{R}_L^l &= \mathbf{H}_{k-1}^H \mathbf{U}_k^l - \mathbf{V}_k^l \text{Diag}(\lambda_k^1, \dots, \lambda_k^l). \end{aligned} \quad (25)$$

The bound (24) is a combined bound. The left-hand side combines the angles for the left and right singular subspace. The right-hand side combines what might be called right and left residuals. The conditions (22) and (23) are separation conditions. The first says that $\lambda_k^1, \dots, \lambda_k^l$ are separated from $\lambda_{k-1}^{l+1}, \dots$. The second condition says that the singular value λ_k^l are separated from the ghost singular values (singular values very close to zero).

In addition to the Wedin theorem, the following inequalities hold [54]

$$\|\mathbf{R}_R^l\| \leq \|\Delta \mathbf{H}_k\|, \|\mathbf{R}_L^l\| \leq \|\Delta \mathbf{H}_k\|. \quad (26)$$

Combining the Wedin theorem and (26), it is clear that, subspaces \mathbf{U}_k^l and \mathbf{V}_k^l are stable, i.e., the angles between \mathbf{U}_k^l and \mathbf{U}_{k-1}^l , plus angles between \mathbf{V}_k^l and \mathbf{V}_{k-1}^l , are bounded by (24), under the conditions (22) and (23). In other words, subspaces \mathbf{V}_k^l and \mathbf{V}_{k-1}^l (subspaces \mathbf{U}_k^l and \mathbf{U}_{k-1}^l) are close to each other.

Similarly, if the separation conditions are satisfied for $l-1$, subspaces \mathbf{V}_k^{l-1} and \mathbf{V}_{k-1}^{l-1} are close to each other. Since $\mathbf{V}_k^l = [\mathbf{V}_k^{l-1} \ \mathbf{v}_k^l]$ and $\mathbf{V}_{k-1}^l = [\mathbf{V}_{k-1}^{l-1} \ \mathbf{v}_{k-1}^l]$, we can say that \mathbf{v}_k^l and \mathbf{v}_{k-1}^l are close, measured by angles between subspaces. Similarly, subspaces \mathbf{u}_k^l and \mathbf{u}_{k-1}^l are close as well.

The bounded angles between subspaces means that, given any \mathbf{v}_{k-1}^l (or \mathbf{u}_{k-1}^l), a vector with bounded Euclidean distance to \mathbf{v}_{k-1}^l (or \mathbf{u}_{k-1}^l) is available in subspace \mathbf{v}_k^l (or \mathbf{u}_k^l).

Concluding the discussion above, when \mathbf{H}_k is assumed nearly flat, \mathbf{U}_k and \mathbf{V}_k that are nearly flat are available, i.e., beamformers of adjacent tones can be bounded in Euclidean distance, if all corresponding singular values satisfy the separation conditions (22) and (23).

V. SMOOTHING OF BEAMFORMERS

In Section IV, the theories show that \mathbf{E}_k , \mathbf{U}_k and \mathbf{V}_k can be bounded in Euclidean distance between adjacent tones, as long as \mathbf{H}_k is nearly flat and the separation conditions are satisfied for singular values of all streams. However, unfortunately, not every SVD algorithm generates \mathbf{U}_k and \mathbf{V}_k 's that are bounded in Euclidean distance across adjacent k 's as required by the proposed architecture. The reason is that: the SVD decomposition is not unique, it may produce more than one set of singular vectors that span the same space but are different [52].

A. Smoothing Criterion and Phase Factor Optimization

To deal with this problem, we propose in this subsection a smoothing criterion and method to smooth the output of any given SVD algorithm so that it satisfies the nearly-flat requirement. The idea here is as follows: We smooth the output of the given SVD algorithm, denoted by $\hat{\mathbf{V}}_k$, to obtain \mathbf{V}_k such that its Euclidean distance to \mathbf{V}_{k-1} is bounded as given in Section IV. The criterion of minimizing the distance of adjacent beamformers is intuitive, due to the fact that Euclidean distance, i.e., Euclidean difference of adjacent vectors, is a measure of first-order smoothness for vector functions. In addition, the criterion is known to be effective thanks to the discussion in Section IV. Running this operation from the beginning to the end of the active frequency tones, a sequence of smoothed beamformers is obtained. It is worth mentioning here that we have also attempted to optimize the second-order smoothness, however no further observable gain over the first-order smoothness optimization was obtained. The reason is that the channel frequency response is rather smooth with the finer beamforming and second-order smoothness or above is unnecessary, under the system parameters and channel models considered in Section VI.

It is assumed that $\hat{\mathbf{v}}_k^l$ is the l -th right singular vector given by the SVD algorithm, corresponding to the singular value $\hat{\lambda}_k^l$ of \mathbf{H}_k , here the hat $\hat{\cdot}$ is to emphasize that $\hat{\mathbf{v}}_k^l$ and $\hat{\lambda}_k^l$ are the outputs of the SVD algorithm before smoothing. Taking $\hat{\mathbf{v}}_k^l$ as the input, after smoothing, \mathbf{v}_k^l is output as the beamformer.

The subspace spanned by $\hat{\mathbf{v}}_k^l$ can be represented by a set $\mathbf{\Pi}(\hat{\mathbf{v}}_k^l) = \{\beta \hat{\mathbf{v}}_k^l e^{j\theta} | \beta \in \mathbb{R}, \theta \in [0, 2\pi)\}$. If $\hat{\lambda}_k^l$ satisfy the separation conditions, distance from $\mathbf{\Pi}(\hat{\mathbf{v}}_k^l)$ to $\mathbf{\Pi}(\mathbf{v}_{k-1}^l)$ is bounded due to the Wedin theorem, here \mathbf{v}_{k-1}^l is the smoothed beamformer of the $(k-1)$ -th frequency tone. Therefore, a vector that has a bounded Euclidean distance to \mathbf{v}_{k-1}^l is available in $\mathbf{\Pi}(\hat{\mathbf{v}}_k^l)$. Then, the problem of smoothing the SVD output is solved by

$$\mathbf{v}_k^l = e^{j\theta^*} \hat{\mathbf{v}}_k^l, \quad (27)$$

where $e^{j\theta^*}$ is a phase factor that minimizes the distance from $e^{j\theta} \hat{\mathbf{v}}_k^l$ to \mathbf{v}_{k-1}^l , i.e.,

$$\theta^* = \arg \min_{\theta} \{ \|e^{j\theta} \hat{\mathbf{v}}_k^l - \mathbf{v}_{k-1}^l\|_2 \}. \quad (28)$$

The solution to the phase factor optimization problem is

$$e^{j\theta^*} = \frac{(\hat{\mathbf{v}}_k^l)^H \mathbf{v}_{k-1}^l}{|(\hat{\mathbf{v}}_k^l)^H \mathbf{v}_{k-1}^l|}. \quad (29)$$

Combining (27) and (29), we have the smoothed output as

$$\mathbf{v}_k^l = \frac{(\hat{\mathbf{v}}_k^l)^H \mathbf{v}_{k-1}^l}{|(\hat{\mathbf{v}}_k^l)^H \mathbf{v}_{k-1}^l|} \hat{\mathbf{v}}_k^l. \quad (30)$$

When two singular values become very close to each other, the bound given by the Wedin theorem is not close to zero even when the channel frequency response is smooth, then smoothness between adjacent beamformers cannot be guaranteed. Still, smoothing is needed to minimize the Euclidean distance of \mathbf{v}_k^l and \mathbf{v}_{k-1}^l for all l 's. While smoothing the SVD output in this case, a special problem needs to be treated carefully. The problem is the ambiguity in pairing one from $\{\hat{\mathbf{v}}_k^1, \dots, \hat{\mathbf{v}}_k^L\}$ with \mathbf{v}_{k-1}^l , which is explained in the following. When $\hat{\lambda}_k^l \approx \lambda_{k-1}^l$ and it is separated from other singular values, there is no doubt that $\hat{\mathbf{v}}_k^l$ should be paired with \mathbf{v}_{k-1}^l . However, when there are multiple singular values of the k -th frequency tone approximate λ_{k-1}^l , i.e., $\hat{\lambda}_k^{l_1} \approx \dots \approx \hat{\lambda}_k^{l_m} \approx \lambda_{k-1}^l$, where m is the number of singular values that are close to λ_{k-1}^l , there has to be a method to determine which of $\hat{\lambda}_k^{l_1}, \dots, \hat{\lambda}_k^{l_m}$ ($\hat{\mathbf{v}}_k^{l_1}, \dots, \hat{\mathbf{v}}_k^{l_m}$) should be paired with λ_{k-1}^l (\mathbf{v}_{k-1}^l), i.e., which one belongs to the l -th stream.

To resolve this ambiguity, we measure the subspace distance from $\hat{\mathbf{v}}_k^{l_i}$ to \mathbf{v}_{k-1}^l , for l_1, \dots, l_m , and select the one with the minimum subspace distance to pair with \mathbf{v}_{k-1}^l . The subspace distance of two vectors, $\hat{\mathbf{v}}_k^{l_i}$ and $\hat{\mathbf{v}}_k^{l_j}$ in our discussion, is defined as [51]

$$d_{l_i} = \| |\hat{\mathbf{v}}_k^{l_i} (\hat{\mathbf{v}}_k^{l_i})^H - \mathbf{v}_{k-1}^l (\mathbf{v}_{k-1}^l)^H \|_2, \quad (31)$$

and let

$$l_* = \arg \min_{l_i \in \{l_1, \dots, l_m\}} \{d_{l_i}\}. \quad (32)$$

Then, $\hat{\lambda}_k^{l_*}$ is taken as the singular value of Stream l , and $\hat{\mathbf{v}}_k^{l_*}$ is smoothed to generate the beamformer as

$$\begin{aligned} \lambda_k^l &= \hat{\lambda}_k^{l_*} \\ \mathbf{v}_k^l &= \frac{(\hat{\mathbf{v}}_k^{l_*})^H \mathbf{v}_{k-1}^l}{|(\hat{\mathbf{v}}_k^{l_*})^H \mathbf{v}_{k-1}^l|} \hat{\mathbf{v}}_k^{l_*}. \end{aligned} \quad (33)$$

B. Smoothing by Orthogonal Iteration

In this subsection, we introduce the orthogonal iteration method [51] for smoothing, which spontaneously follows the proposed smoothing criterion due to its iterative nature. Compared with the phase factor optimization method, the orthogonal iteration enjoys lower computational complexity. The orthogonal iteration method has been used in [52] to provide smooth beamforming for an OFDM system to enable channel state information (CSI) smoothing.

As we know, \mathbf{V}_k is the right singular vectors of \mathbf{H}_k , as well as the eigenvectors of $\mathbf{A}_k = \mathbf{H}_k^H \mathbf{H}_k$, which can be found by performing the following iteration from an initial matrix $\mathbf{Q}^{(0)} \in \mathbb{C}^{N_t \times L}$ with orthonormal columns

$$\mathbf{B}^{(i)} = \mathbf{A}_k \mathbf{Q}^{(i-1)}, \quad i = 1, 2, \dots \quad (34)$$

QR decomposition: $\mathbf{B}^{(i)} = \mathbf{Q}^{(i)} \mathbf{R}^{(i)}$,

where i denotes the iteration index and N_{iter} is the total number of iterations. According to [52], $\mathbf{R}^{(i)}$ converges to a diagonal matrix containing the eigenvalues of \mathbf{A}_k , and $\mathbf{Q}^{(i)}$ converges to an orthonormal basis for the dominant subspace of dimension L .

For a beamforming that is smooth from Tone $k-1$ to k , \mathbf{V}_{k-1} could serve as the initial $\mathbf{Q}^{(0)}$, and the output is $\mathbf{V}_k = \mathbf{Q}^{(N_{\text{iter}})}$. It will be shown in the next section that very few iterations are needed to obtain a satisfactory \mathbf{V}_k , which ensures smoothness from \mathbf{V}_{k-1} to \mathbf{V}_k . The complete algorithm is presented in Algorithm 1.

Algorithm 1: Orthogonal Iteration for Smooth Beamforming

- 1: Initialize $\mathbf{V}_0 = \text{SVD}(\mathbf{H}_0)$ (SVD(\cdot) stands for an arbitrary SVD algorithm);
 - 2: **for** $k = 1 : KM - 1$ **do**
 - 3: $\mathbf{A}_k = \mathbf{H}_k^H \mathbf{H}_k$;
 - 4: $\mathbf{V}_k = \mathbf{V}_{k-1}$;
 - 5: **for** $i = 1 : N_{\text{iter}}$ **do**
 - 6: $\mathbf{B}_k = \mathbf{A}_k \mathbf{V}_k$;
 - 7: Update \mathbf{V}_k using the following QR decomposition:
 $\mathbf{B}_k = \mathbf{V}_k \mathbf{R}_k$;
 - 8: **end for**
 - 9: $\mathbf{D}_k = \text{SQRT}(\mathbf{R}_k)$ (SQRT(\cdot) stands for the square root of an diagonal matrix);
 - 10: **end for**
-

VI. SIMULATION RESULTS

In this section, we evaluate the performance of the finer and smoothed SVD beamforming for FBMC/OQAM that was proposed in this paper, through computer simulations. We compare the proposed SVD-FS-FBMC system with an SVD-OFDM system, under a setup similar to the IEEE 802.11n wireless LAN standard. Thanks to orthogonality among subchannels, the error performance of SVD-OFDM is the upper bound of the proposed SVD-FS-FBMC, if the CP overhead of OFDM is ignored. The presented results reveal excellent performance of our proposed method, which can compete with OFDM and give close BER results with 64-QAM constellation, under channel models of the IEEE 802.11n standard. As shown by Table I, the Channel Model D, E, and F of the IEEE 802.11n standard have relatively large maximum delay spread, when normalized by the OFDM symbol duration (3200ns), which result in strong frequency selectivity. Especially for the Channel Model F, the maximum delay spread is even longer than the CP defined in the standard (800ns).

For the simulations presented in this section, the following parameters are used for both SVD-FS-FBMC and SVD-OFDM systems. The MIMO system is configured as $N_t =$

TABLE I
MAXIMUM DELAY SPREAD OF THE CHANNEL MODELS

Channel Model	Maximum delay spread (ns)	Maximum delay spread normalized by the OFDM symbol duration
D	390	12.2%
E	730	22.8%
F	1050	32.8%

$N_r = L = 2$. There are $M = 64$ subcarriers, and the subcarrier spacing is 312.5 kHz. Among the 64 subcarriers, 48 are active subcarriers modulated with 16-QAM or 64-QAM constellations. We apply no power allocation among subcarriers and streams in the simulation, i.e., all streams (and 48 subcarriers) have equal transmit power. For channel coding, we use convolutional code of rate 2/3 and constraint length 7. A random interleaver is applied after the coding. Each data frame consists of 7 FBMC/OFDM symbols (each consists of 48 OQAM/QAM symbols). The FBMC systems employ the PHYDYAS filter [53], and the overlapping factor K is 4. With the FFT size of $4M$, the filter has 7 non-negligible tones, i.e., $P = 4$. For the singular value equalization, a ZF equalizer is employed at receiver of the proposed SVD-FS-FBMC. And, we set $N_{\text{iter}} = 3$ for the orthogonal iteration method. The SNR in the simulation is defined as: $\text{SNR} \triangleq N_t \sigma_a^2 \sigma_h^2 / \sigma_n^2$, where σ_a^2 , σ_h^2 and σ_n^2 are the expected signal power of each transmit antenna, expected channel power gain between a pair of transmit and receive antennas, and expected AWGN noise power of each receive antenna, respectively, on each active subchannel.

In most of the following figures, we present the performance of the proposed SVD-FS-FBMC system with the orthogonal iteration of three iterations. To justify the use of orthogonal iteration and $N_{\text{iter}} = 3$, BER performance comparison between the orthogonal iteration of different iterations and phase factor optimization is presented in Section VI-C, followed by complexity comparison of these proposed smoothing methods.

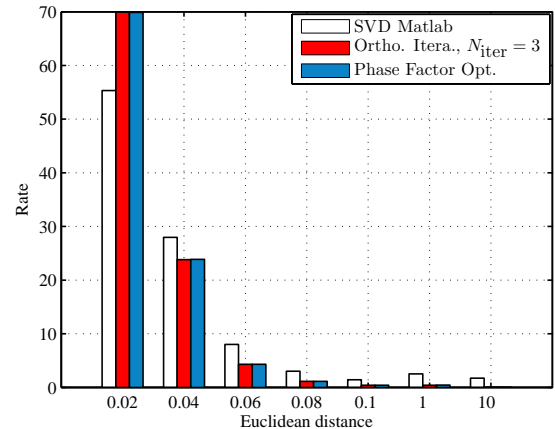


Fig. 4. The Euclidean distance between transmit beamformers of adjacent tones.

A. Smoothness of Beamformers

Let us first check if the smoothness across tones is improved with the proposed smoothing methods introduced in Section V. Smoothness between two beamformers of adjacent tones is measured by their Euclidean difference. Fig. 4 presents the histogram of the Euclidean distance between adjacent beamformers by the proposed methods. Result by the SVD function in the Matlab software is also presented for comparison. The distance of the proposed schemes falls in the range of $0 \sim 1.0$, while that of SVD Matlab could go beyond 1.0 with non-negligible percentage. It is thus concluded that the phase factor optimization and the orthogonal iteration method provide significant smoothness improvements compared with the SVD of no smoothness consideration. It is also observed that there is no observable difference in the histogram between the phase factor optimization and orthogonal iteration with $N_{\text{iter}} = 3$, which verifies the ability of the orthogonal iteration to fulfill the proposed smoothing criterion spontaneously.

B. The BER Performance

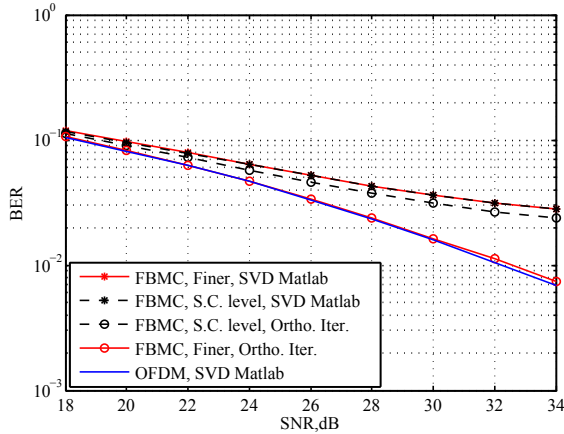


Fig. 5. BER performance of the SVD-FS-FBMC systems with 64-QAM and no coding, subchannel level or finer beamforming, orthogonal iteration or Matlab SVD, Channel Model D, $N_{\text{iter}} = 3$.

TABLE II
SUMMARY OF THE SCHEMES UNDER COMPARISON

Schemes	Beamforming granularity	Smoothing
SVD-OFDM	S.C. level	SVD Matlab (No smoothing)
Basic SVD-FBMC/OQAM	S.C. level	SVD Matlab (No smoothing)
SVD-FBMC/OQAM w/ smoothing	S.C. level	Ortho. Iter. (Smoothing)
SVD-FS-FBMC w/o smoothing	Finer	SVD Matlab (No smoothing)
Proposed SVD-FS-FBMC	Finer	Ortho. Iter. (Smoothing)

The simulation results in this subsection mainly demonstrate the performance of the orthogonal iteration method, the comparison between the orthogonal iteration method and the phase factor optimization method is presented in Subsection

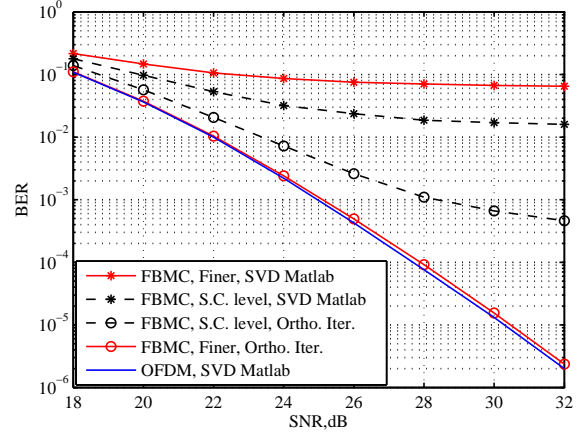


Fig. 6. BER performance of the SVD-FS-FBMC systems with 64-QAM and rate 2/3 coding, subchannel level or finer beamforming, orthogonal iteration or Matlab SVD, Channel Model D, $N_{\text{iter}} = 3$.

VI-C. Fig. 5 and 6 present BER performance of the SVD-FS-FBMC system with the proposed finer beamforming and smoothing under Channel Model D, without and with coding, respectively. For comparison, we also present BER results of the following four systems: i) SVD-OFDM; ii) Basic SVD-FBMC/OQAM with subchannel-level (S.C. level) beamforming and without smoothing (SVD Matlab), this is the straightforward combination of SVD and FBMC/OQAM discussed in Section II; iii) SVD-FBMC/OQAM with subchannel-level beamforming and smoothing (orthogonal iteration), its performance gap to the proposed SVD-FS-FBMC shows how the proposed beamforming with finer granularity improves the performance; iv) SVD-FS-FBMC with the finer beamforming but without smoothing (SVD Matlab), its performance gap to the proposed SVD-FS-FBMC shows how the proposed smoothing improves the performance. The schemes under comparison are summarized in Table II. The simulations of Fig. 5 and 6 demonstrate that both beamforming with finer granularity and smoothing are necessary for a good beamforming of FBMC system under frequency selective channels. The results clearly show that the SVD-FS-FBMC system with the proposed finer beamforming and smoothing greatly outperforms the other SVD-FBMC/OQAM and SVD-FS-FBMC systems. And it performs very closely with SVD-OFDM, in terms of BER, under the IEEE 802.11n Channel Model D. It is also observed that smoothing is crucial for the BER performance: the subchannel-level SVD-FBMC/OQAM systems with smoothing outperforms the SVD-FBMC/OQAM without smoothing. One may notice that the system with finer beamforming but no smoothing has the worst BER performance among the systems in comparison. The reason is that, when finer beamforming is employed without smoothing, significant changes of beamformer may happen between two tones of one subcarrier band, which results in serious distortion of the transmitted signal.

Performance of the proposed scheme is also evaluated under channels of more frequency selectivity, i.e., Channel Model E and F, with 2/3 coding, for 64-QAM and 16-

QAM modulation, respectively in Fig. 7 and Fig. 8. As the channel selectivity increases, error floor is observed for FBMC systems. Employing lower-order modulation reduces the performance gap between the proposed SVD-FS-FBMC and SVD-OFDM, however does not stop it from growing at high SNRs under the Channel Model F.

In the simulation of Fig. 9, we increase the FFT size to $8M$ and test the proposed SVD-FS-FBMC under channel Model F. Increasing the FFT size from $4M$ to $8M$ doubles the number of frequency tones of the FS-FBMC receiver, and therefore gives even finer beamforming, at the cost of doubled complexity. As observed from Fig. 9, performance of the proposed SVD-FS-FBMC is improved at high SNRs and close to that of SVD-OFDM.

It should be noted that the BER plots above is with respect to SNR. If we use E_b/N_0 instead of SNR for x-axis, about 1 dB gain of the proposed SVD-FS-FBMC will be observed over SVD-OFDM, because that the SVD-FS-FBMC does not pay for the energy overhead to transmit the 25% cyclic prefix as the OFDM in IEEE 802.11n does.

C. Computational complexity of the proposed smoothing methods

In this subsection, we examine the number of iterations required for the smoothing of orthogonal iteration and then give a complexity comparison between the phase factor optimization and orthogonal iteration.

The BER performance of the proposed SVD-FS-FBMC system with orthogonal iteration is presented for different number of iterations in Fig. 10, with 2/3 coding, 64-QAM modulation, various channel models. Performance of phase factor optimization is also presented for comparison. As observed from Fig. 10, $N_{\text{iter}} = 3$ is adequate for the orthogonal iteration method to achieve a similar performance as the phase factor optimization under Channel Model D, E and F. For channel model with less frequency selectivity, such as Channel Model D and E, the number of iterations could be further reduced.

We express the computational complexity in terms of the number of floating point operations (FLOPS) [57]. Each scalar/complex addition or multiplication is counted as one FLOPS. Table III shows the complexity of operations in smoothed SVD with orthogonal iteration [57]. Assuming $N_{\text{iter}} = 3$ and $N_t = N_r$, the total complexity of the orthogonal iteration for each frequency tone is $13N_t^3 - \frac{5}{2}N_t^2 - \frac{1}{2}N_t$ FLOPS. Omitting the small order terms, the complexity is $13N_t^3$ FLOPS for each frequency tone. For the phase factor optimization method, the major complexity of each frequency tone is the direct computation of SVD from the channel matrix \mathbf{H}_k , which is about $4N_t^2N_r + 8N_tN_r^2 + 9N_r^3$ FLOPS as given in [58]. Assuming $N_t = N_r$, the complexity of the phase factor optimization is $21N_t^3$ FLOPS for each frequency tone, which is higher than that of the orthogonal iteration with three iterations.

VII. CONCLUSIONS

This paper proposed a scheme and a couple of methods to combine SVD beamforming and FBMC/OQAM. Simulation

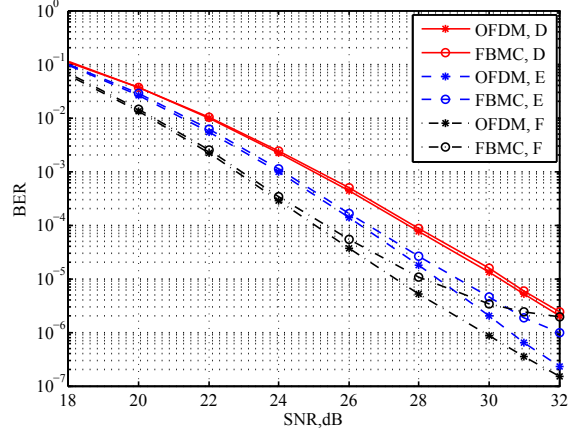


Fig. 7. BER performance of the proposed SVD-FS-FBMC system with 64-QAM and rate 2/3 coding, channel Model D, E, and F, $N_{\text{iter}} = 3$.

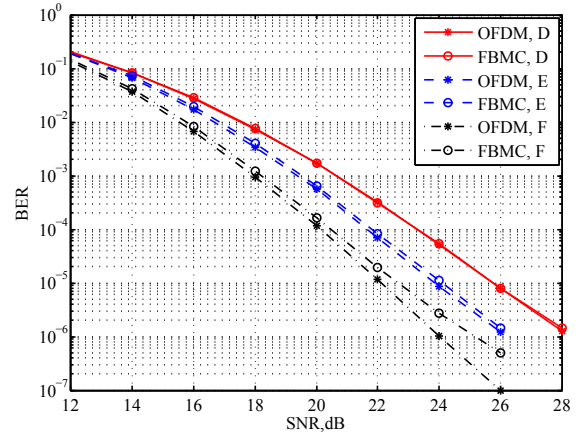


Fig. 8. BER performance of the proposed SVD-FS-FBMC system with 16-QAM and rate 2/3 coding, channel Model D, E, and F, $N_{\text{iter}} = 3$.

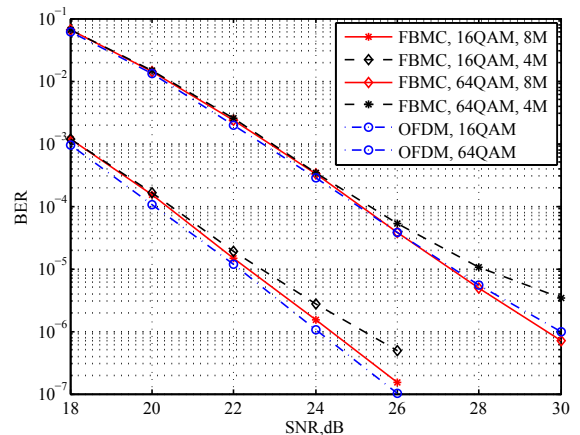


Fig. 9. BER performance of the proposed SVD-FS-FBMC systems with 16 and 64-QAM, rate 2/3 coding, FFT size $4M$ and $8M$, $N_{\text{iter}} = 3$, Channel Model F.

TABLE III
COMPLEXITY OF OPERATIONS IN SMOOTHED SVD WITH ORTHOGONAL ITERATION.

Operations	Complexity (FLOPS)
$\mathbf{A}_k = \mathbf{H}_k^H \mathbf{H}_k$	$N_t^2 N_r + N_t N_r - \frac{1}{2} N_t^2 - \frac{1}{2} N_t$
$\mathbf{B}_k = \mathbf{A}_k \mathbf{V}_k$, N_{iter} times	$(2N_t^3 - N_t^2) N_{\text{iter}}$
QR decomposition: $\mathbf{B}_k = \mathbf{V}_k \mathbf{R}_k$, N_{iter} times	$(\frac{4}{3} N_t^3) N_{\text{iter}}$
Calculation of \mathbf{U}_k from $\mathbf{H}_k = \mathbf{U}_k \mathbf{D}_k \mathbf{V}_k^H$	$2N_t^2 N_r$

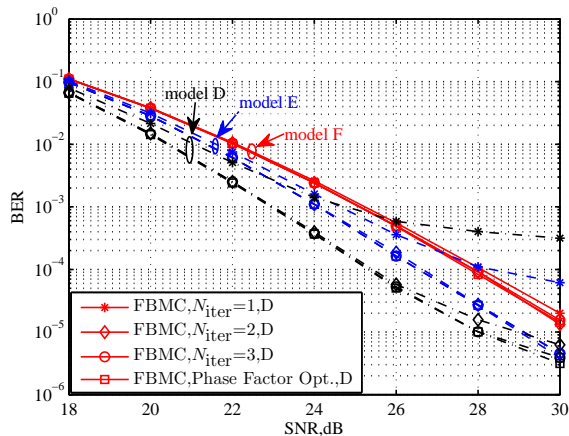


Fig. 10. BER performance of the proposed SVD-FS-FBMC system with 64-QAM and rate 2/3 coding, FFT size $4M$, Channel Model F, $N_{\text{iter}} = 1, 2, 3$ and 10.

results show that the proposed SVD-FS-FBMC system shares close BER performance with its OFDM counterpart under the IEEE 802.11n Channel Models. The excellent performance comes from two aspects that greatly improve the smoothness of beamformers: i) beamforming with finer granularity in frequency domain; ii) smoothing the beamformers from tone to tone.

Although the orthogonal iteration reduces the complexity of SVD decomposition to certain level, it is still quite a computational burden when the number of antennas and streams is large. In the future, lower-complexity beamforming schemes and tradeoff between error performance and computational complexity are to be studied.

APPENDIX

In this appendix, we prove (19) under the nearly-flat assumptions on \mathbf{H}_k , \mathbf{V}_k , \mathbf{E}_k , and \mathbf{U}_k . Let (18) be rewritten as

$$\begin{aligned} & \tilde{\mathbf{a}}_{m_0, n_0} \\ &= \mathbf{c}_{m_0, n_0} + \sum_{(m, n) \neq (m_0, n_0)} \mathbf{c}_{m, n} \\ & \quad + \sum_{k=0}^{KM-1} G_{m_0, n_0}^{(n_0)*}(k) \mathbf{E}_k \mathbf{U}_k^H \mathbf{n}^{(n_0)}(k), \end{aligned} \quad (35)$$

where $\mathbf{c}_{m, n}$ represents the contribution of $\mathbf{a}_{m, n}$ to $\tilde{\mathbf{a}}_{m_0, n_0}$. Then, our goal in this appendix is to prove $\mathbf{c}_{m, n} \approx \mathbf{a}_{m, n} \zeta_{m, n}^{m_0, n_0}$ so that (19) holds.

Combining (18) and (35), we have

$$\mathbf{c}_{m, n} = \sum_{k=0}^{KM-1} G_{m_0, n_0}^{(n_0)*}(k) \mathbf{E}_k \mathbf{U}_k^H \tilde{\mathbf{b}}_{m, n}^{(n_0)}(k), \quad (36)$$

where $\tilde{\mathbf{b}}_{m, n}^{(n_0)}(k)$ denote the part of $\tilde{\mathbf{b}}^{(n_0)}(k)$ that is contributed by $\mathbf{a}_{m, n}$.

Due to the assumption that \mathbf{E}_k and \mathbf{U}_k are nearly flat across the subcarrier band, the term $G_{m_0, n_0}^{(n_0)*}(k) \mathbf{E}_k \mathbf{U}_k^H$ in (36) can be approximated for k around Km_0 as

$$G_{m_0, n_0}^{(n_0)*}(k) \mathbf{E}_k \mathbf{U}_k^H \approx G_{m_0, n_0}^{(n_0)*}(k) \mathbf{E}_{Km_0} \mathbf{U}_{Km_0}^H, \quad (37)$$

which then corresponds to $g_{m_0, n_0}^*(i) \mathbf{E}_{Km_0} \mathbf{U}_{Km_0}^H$ in time domain.

On the other hand, at the transmitter, the beamformed signals on all antennas is given in frequency domain by

$$\mathbf{b}_{m, n}(k) = \mathbf{V}_k \mathbf{a}_{m, n} G_{m, n}^{(n)}(k). \quad (38)$$

It corresponds to $\mathbf{x}_{m, n}(i)$ in time domain, which is defined as

$$\mathbf{x}_{m, n}(i) = \begin{cases} \sum_{k=0}^{KM-1} \mathbf{b}_{m, n}(k) e^{j \frac{2\pi k(i - nM/2)}{KM}}, & \frac{nM}{2} \leq i \leq \frac{nM}{2} + KM - 1 \\ 0, & \text{else} \end{cases} \quad (39)$$

Due to the assumption that \mathbf{V}_k is nearly flat across the subcarrier band,

$$\mathbf{b}_{m, n}(k) \approx \mathbf{V}_{Km} \mathbf{a}_{m, n} G_{m, n}^{(n)}(k), \quad (40)$$

and it corresponds to

$$\mathbf{x}_{m, n}(i) \approx \mathbf{V}_{Km} \mathbf{a}_{m, n} g_{m, n}(i). \quad (41)$$

Due to the assumption that \mathbf{H}_k is nearly flat across the subcarrier band, the signals on all receive antennas that are contributed by $\mathbf{a}_{m, n}$ is

$$\mathbf{y}_{m, n}(i) \approx \mathbf{H}_{Km} \mathbf{x}_{m, n}(i) \approx \mathbf{H}_{Km} \mathbf{V}_{Km} \mathbf{a}_{m, n} g_{m, n}(i). \quad (42)$$

Taking the note that $\tilde{\mathbf{b}}_{m, n}^{(n_0)}(k)$ is the FFT of the part of $\mathbf{y}_{m, n}(i)$ falling into the n_0 -th window, and using (37) and

(42), (36) is rewritten in time domain as

$$\begin{aligned}
\mathbf{c}_{m,n} &= \sum_{k=0}^{KM-1} G_{m_0,n_0}^{(n_0)*}(k) \mathbf{E}_k \mathbf{U}_k^H \tilde{\mathbf{b}}_{m,n}^{(n_0)}(k) \\
&\approx \sum_{i=\frac{n_0 M}{2}}^{\frac{n_0 M}{2} + KM - 1} g_{m_0,n_0}^*(i) \mathbf{E}_{Km_0} \mathbf{U}_{Km_0}^H \mathbf{y}_{m,n}(i) \\
&= \sum_{i=-\infty}^{+\infty} g_{m_0,n_0}^*(i) \mathbf{E}_{Km_0} \mathbf{U}_{Km_0}^H \mathbf{y}_{m,n}(i) \\
&\approx \sum_{i=-\infty}^{+\infty} g_{m_0,n_0}^*(i) \mathbf{E}_{Km_0} \mathbf{U}_{Km_0}^H \mathbf{H}_{Km} \mathbf{V}_{Km} \mathbf{a}_{m,n} g_{m,n}(i).
\end{aligned} \tag{43}$$

Clearly, $\mathbf{c}_{m,n}$ is non-zero only when $g_{m_0,n_0}^*(i)$ and $g_{m,n}(i)$ overlap in frequency, which means that frequency tone Km_0 and Km are within the width of one subcarrier band. Taking use of the nearly-flat assumption, we replace \mathbf{E}_{Km_0} and $\mathbf{U}_{Km_0}^H$ in (43) by \mathbf{E}_{Km} and \mathbf{U}_{Km}^H , respectively. Finally, using the relations that $\mathbf{U}_k^H \mathbf{H}_k \mathbf{V}_k = \mathbf{D}_k$ and $\mathbf{E}_k \mathbf{D}_k = \mathbf{I}_L$ (assuming the ZF equalization of singular values), we arrive at

$$\mathbf{c}_{m,n} \approx \mathbf{a}_{m,n} \zeta_{m,n}^{m_0,n_0}. \tag{44}$$

Specifically, $\mathbf{c}_{m_0,n_0} \approx \mathbf{a}_{m_0,n_0}$.

REFERENCES

- [1] B. Farhang-Boroujeny, "OFDM versus filter bank multicarrier," *IEEE Signal Processing Magazine*, vol. 28, no. 3, pp. 92-112, May 2011.
- [2] P. Siohan, C. Siclet, and N. Lacaille, "Analysis and design of OQAM/OFDM systems based on filterbank theory," *IEEE Transactions on Signal Processing*, vol. 50, no. 5, pp. 1170-1183, May 2002.
- [3] B. Hirotsaki, "An orthogonally multiplexed QAM system using the discrete Fourier transform," *IEEE Transactions on Communications*, vol. 29, no. 7, pp. 982-989, Jul. 1981.
- [4] T. Ihalainen, A. Ikhlef, J. Louveaux, and M. Renfors, "Channel Equalization for Multi-Antenna FBMC/OQAM Receivers," *IEEE Transactions on Vehicular Technology*, vol. 60, no. 5, pp. 2070-2085, Jun. 2011.
- [5] X. Gao, W. Wang, X. Xia, E. K. S. Au, and X. You, "Cyclic prefixed OQAM-OFDM and its application to single-carrier FDMA," *IEEE Transactions on Communications*, vol. 59, no. 5, pp. 1467-1480, May 2011.
- [6] D. Chen, D. Qu, T. Jiang, and Y. He, "Prototype filter optimization to minimize stopband energy with NPR constraint for filter bank multicarrier modulation systems," *IEEE Transactions on Signal Processing*, vol. 61, no. 1, pp. 159-169, Jan. 2013.
- [7] H. Zhang, D. Le Ruyet, D. Roviras, and H. Sun, "Noncooperative multicell resource allocation of FBMC-based cognitive radio systems," *IEEE Transactions on Vehicular Technology*, vol. 61, no. 2, pp. 799-811, Feb. 2012.
- [8] W. Wang, X. Gao, F. Zheng, and W. Zhong, "CP-OQAM-OFDM based SC-FDMA: adjustable user bandwidth and space-time coding," *IEEE Transactions on Wireless Communications*, vol. 12, no. 9, pp. 4506-4517, Sep. 2013.
- [9] D. Qu, S. Lu, and T. Jiang, "Multi-block joint optimization for the peak-to-average power ratio reduction of FBMC-OQAM signals," *IEEE Transactions on Signal Processing*, vol. 61, no. 7, pp. 1605-1613, Apr. 2013.
- [10] W. Cui, D. Qu, T. Jiang, and B. Farhang-Boroujeny, "Coded auxiliary pilots for channel estimation in FBMC-OQAM systems," *IEEE Transactions on Vehicular Technology*, vol. 65, no. 5, pp. 2936-2946, May 2016.
- [11] L. Zhang, P. Xiao, A. Zafar, A. ul Qudus and R. Tafazolli, "FBMC System: An Insight into Doubly Dispersive Channel Impact," *IEEE Transactions on Vehicular Technology*.
- [12] H. Lee, B. Kwon, D. Jeon, S. Kim, and S. Lee, "Mutual Interference Analysis of FBMC based Return Channel for Bidirectional T-DMB System," *IEEE Transactions on Vehicular Technology*.
- [13] R. Chang, and R. Gibbey, "A theoretical study of performance of an orthogonal multiplexing data transmission scheme," *IEEE Transactions on Communication Technology*, vol. 16, no. 4, pp. 529-540, Aug. 1968.
- [14] W. Y. Zou, and Y. Wu, "COFDM: An overview," *IEEE Transactions on Broadcasting*, vol. 41, no. 1, pp. 1-8, Mar. 1995.
- [15] I. Estella, A. Pascual-Iserte, and M. Payaro, "OFDM and FBMC performance comparison for multistream MIMO systems," *Future Network and Mobile Summit*, pp. 1-8, Jun. 2010.
- [16] M. Caus, and A. I. Perez-Neira, "Transmitter-Receiver Designs for Highly Frequency Selective Channels in MIMO FBMC Systems," *IEEE Transactions on Signal Processing*, vol.60, no.12, pp.6519-6532, Dec. 2012.
- [17] M. Caus, and A. I. Perez-Neira, "Multi-Stream Transmission for Highly Frequency Selective Channels in MIMO-FBMC/OQAM Systems," *IEEE Transactions on Signal Processing*, vol.62, no.4, pp.786-796, Feb. 2014.
- [18] Y. Cheng, P. Li, and M. Haardt, "Coordinated beamforming in MIMO FBMC/OQAM systems," *IEEE International Conference on Speech and Signal Processing (ICASSP)*, pp.484-488, May 2014.
- [19] M. Caus, A. I. Perez-Neira, Y. Cheng, and M.Haardt, "Towards a non-error floor multi-stream beamforming design for FBMC/OQAM," *IEEE International Conference on Communications (ICC)*, pp.4763-4768, Jun. 2015.
- [20] M. Caus, and A. I. Perez-Neira, "Multi-stream transmission in MIMO-FBMC systems," *IEEE International Conference on Speech and Signal Processing (ICASSP)*, pp.5041-5045, May 2013.
- [21] X. Mestre, and D. Gregoratti, "Parallelized Structures for MIMO FBMC Under Strong Channel Frequency Selectivity," *IEEE Transactions on Signal Processing*, vol. 64, no. 5, pp. 1200-1215, Mar. 2016.
- [22] X. Mestre, and D. Gregoratti, "Eigenvector precoding for FBMC modulations under strong channel frequency selectivity," *IEEE International Conference on Communications (ICC)*, pp.4769-4774, Jun. 2015.
- [23] O. D. Candido, L. G. Baltar, A. Mezghani, and J. A. Nossek, "SIMO/MISO MSE-Duality for Multi-User FBMC with Highly Frequency Selective Channels," *19th International ITG Workshop on Smart Antennas*, Mar. 2015.
- [24] M. Newinger, L. G. Baltar, A. L. Swindlehurst, and J. A. Nossek, "MISO Broadcasting FBMC System for Highly Frequency Selective Channels," *18th International ITG Workshop on Smart Antennas*, Mar. 2014.
- [25] Y. Cheng, V. Ramireddy, and M. Haardt, "Non-linear precoding for the downlink of FBMC/OQAM based multi-user MIMO systems," *19th International ITG Workshop on Smart Antennas*, Mar. 2015.
- [26] A. I. Perez-Neira, M. Caus, R. Zakaria, D. Le Ruyet, E. Kofidis, M. Haardt, X. Mestre, and Y. Cheng, "MIMO Signal Processing in Offset-QAM Based Filter Bank Multicarrier Systems," *IEEE Transactions on Signal Processing*, vol. 64, no. 21, pp. 5733-5762, June 2016.
- [27] F. Harris, C. Dick, and M. Rice, "Digital receivers and transmitters using polyphase filter banks for wireless communications," *IEEE Transactions on Microwave Theory and Technology*, vol. 51, no. 4, pp. 1395C1412, Apr. 2003.
- [28] M. G. Bellanger, "FBMC physical layer: A primer," Available <http://www.ictphydyas.org/team-space/internal-folder/FBMCPrimer06-2010.pdf>.
- [29] E. Perahia, and R. Stacey, *Next Generation Wireless LANs: Throughput, Robustness, and Reliability in 802.11n*. Cambridge, UK: Cambridge University Press, 2008.
- [30] M. Bellanger, "FS-FBMC: an alternative scheme for filter bank based multicarrier transmission," *5th International Symposium on Communications Control and Signal Processing (ISCCSP)*, pp.1-4, May 2012.
- [31] D. Mattered, M. Tanda, and M.Bellanger, "Analysis of an FBMC/OQAM scheme for asynchronous access in wireless communications," *EURASIP Journal on Advances in Signal Processing*, vol. 2015, no. 1, Dec. 2015.
- [32] J.-B. Dore, V. Berg, N. Cassiau, and D. Ktenas, "FBMC receiver for multi-user asynchronous transmission on fragmented spectrum," *EURASIP Journal on Advances in Signal Processing*, vol. 41, Mar. 2014.
- [33] D. Mattered, M. Tanda, and M. Bellanger, "Frequency domain CFO compensation for FBMC systems," *Signal Processing*, vol. 114, pp. 183-197, 2015.
- [34] D. Qu, Y. Qiu, and T. Jiang, "Finer SVD-based Beamforming for FBMC/OQAM systems," *IEEE Globecom*, Washington, DC, USA, Dec. 2016.
- [35] J.-B. Dore, R. Gerzaguet, N. Cassiau, and D. Ktenas, "Waveform contenders for 5G: Description, analysis and comparison," *Physical Communication*, vol. 24, pp. 46-61, Sep. 2017.
- [36] J.-B. Dore, V. Berg and D. Ktenas, "Channel estimation techniques for 5G cellular networks: FBMC and multiuser asynchronous fragmented spectrum scenario," *Transactions on Emerging Telecommunications Technologies*, vol. 26, no. 1, pp. 15-30, Jan. 2015.

- [37] A. Aminjavaheri, A. Farhang, N. Marchetti, L. Doyle, and B. Farhang-Boroujeny, "Frequency Spreading Equalization in multicarrier Massive MIMO" *IEEE International Conference on Communication Workshop*, Jun. 2015.
- [38] Y. Won, J. Oh, J. Lee, and J. Kim, "A Study of an Iterative Channel Estimation Scheme of FS-FBMC System," *Wireless Communications and Mobile Computing*, vol. 2017, Jan. 2017.
- [39] J. Nadal, C. Nour, and A. Baghdadi, "Design and Evaluation of a Novel Short Prototype Filter for FBMC/OQAM Modulation," *IEEE Access*, DOI: 10.1109/ACCESS.2018.2818883, Mar. 2018.
- [40] D. Mattera, M. Tanda, M. Bellangerb, "Performance analysis of some timing offset equalizers for FBMC/OQAM systems," *Signal Processing*, vol. 108, pp. 167-182, Mar. 2015.
- [41] M. Carvalho, M. Ferreira, and J. Ferreira, "FPGA-based Implementation of a Frequency Spreading FBMC-OQAM Baseband Modulator," *24th IEEE International Conference on Electronics, Circuits and Systems (ICECS)*, Dec. 2017.
- [42] C. L  l  , J. P. Javaudin, R. Legouable, A. Skrzypczak, and P. Siohan, "Channel estimation methods for preamble-based OFDM/OQAM modulations," *European Wireless Conference*, pp. 59-64, Mar. 2007.
- [43] G. Lebrun, J. Gao, and M. Faulkner, "MIMO transmission over a time-varying channel using SVD," *IEEE Transactions on Wireless Communications*, vol. 4, no. 2, pp. 757-764, Mar. 2005.
- [44] M. L. Boucheret, I. Mortensen, and H. Favaro, "Fast convolution filter banks for satellite payloads with on-board processing," *IEEE Journal on Selected Areas in Communications*, vol. 17, no. 2, pp. 238-248, Feb. 1999.
- [45] C. Zhang, and Z. Wang, "A fast frequency domain filter bank realization algorithm," *5th International Conference on Signal Processing Proceedings*, pp. 130-132, Aug. 2000.
- [46] L. Pucker, "channelization techniques for software defined radio," *Proceedings of SDR Forum Conference*, pp. 1-6, Nov. 2003.
- [47] M. Umehira, and M. Tanabe, "Performance analysis of overlap FFT filter-bank for dynamic spectrum access applications," *2010 16th Asia-Pacific Conference on Communications*, pp. 424-428, Oct. 2010.
- [48] M. Renfors, and F. Harris, "Highly adjustable multirate digital filters based on fast convolution," *2011 20th European Conference on Circuit Theory and Design*, pp. 9-12, Aug. 2011.
- [49] M. Renfors, J. Yli-Kaakinen, and F. J. Harris, "Analysis and design of efficient and flexible fast-convolution based multirate filter banks," *IEEE Transactions on Signal Processing*, vol. 15, no. 62, pp. 3768-3783, Aug. 2014
- [50] V. Berg, J.-B. Dore, and D. Noguet, "A flexible FS-FBMC receiver for dynamic access in the TVWS," *IEEE Vehicular Technology Conference Cognitive Radio Oriented Wireless Networks and Communications (CROWNCOM)*, pp.285-290, Jun. 2014.
- [51] G. Golub, and C. van Loan, *Matrix Computations*. Johns Hopkins University Press, 3rd ed., 1996.
- [52] M. Sandell, and V. Ponnampalam, "Smooth beamforming for OFDM," *IEEE Transactions on Wireless Communications*, vol. 8, no. 3, pp. 1133-1138, Mar. 2009.
- [53] A. Viholainen, M. Bellanger, and M. Huchard, "Prototype filter and structure optimization," Available: <http://www.ict-phydyas.org/delivrables/PHYDYAS-D5-1.pdf/view>.
- [54] G. W. Stewart, "Perturbation Theory for the Singular Value Decomposition," *UMIACS-TR-90-124, CS-TR 2539*, September 1990.
- [55] H. Weyl, "Das asymptotische verteilungsgesteuerte der Eigenwert linearer partieller differentialgleichungen (mit einer Anwendung auf der theorie der hohlraumstrahlung)," *Math. Annalen*, vol. 71, pp. 441-479, 1912.
- [56] P. A. Wedin, "Perturbation bounds in connection with singular value decomposition," *BIT*, vol. 12, pp. 99-111, 1972.
- [57] R. Hunger, "Floating Point Operations in Matrix-Vector Calculus," Technische Universit  t M  nchen, Associate Institute for Signal Processing, Tech. Rep., 2007.
- [58] R. A. Horn and C. R. Johnson, *Matrix Analysis*. Cambridge university press, 2012.